

Importance of dispersion in density functional calculations of cesium chloride and its related halidesF. Zhang,^{1,*} J. D. Gale,¹ B. P. Uberuaga,² C. R. Stanek,² and N. A. Marks³¹*Nanochemistry Research Institute, Department of Chemistry, Curtin University, P.O. Box U1987, Perth, Western Australia 6845, Australia*²*Material Science and Technology Division, Los Alamos National Laboratory, Los Alamos, New Mexico 87545, USA*³*Nanochemistry Research Institute, Discipline of Physics and Astronomy, Curtin University, P.O. Box U1987, Perth, Western Australia 6845, Australia*

(Received 12 June 2013; published 19 August 2013)

The ionic compound cesium chloride adopts a cubic crystal structure bearing the same name. However, *ab initio* electronic structure calculations based on density functional theory methods using generalized gradient approximation functionals do not predict that cesium chloride adopts this phase. In this paper we apply semiempirical methods (density functional theory plus a pairwise dispersion correction) to account for missing van der Waals interactions within cesium chloride. The C_6 and R_0 dispersion parameters for cesium are established within Grimme's DFT + D2 formalism. Inclusion of the dispersion corrections is found not only to improve the quality of structures in comparison to experiment for all cesium halides, but also leads to the correct prediction of the ground-state phase under ambient conditions.

DOI: [10.1103/PhysRevB.88.054112](https://doi.org/10.1103/PhysRevB.88.054112)

PACS number(s): 31.15.E-, 61.66.Fn, 61.50.Lt, 71.20.-b

I. INTRODUCTION

It is widely assumed that the alkali-metal halides represent simple model systems that are well understood and require little further exploration by quantum mechanical methods. Most alkali-metal halides adopt the rocksalt NaCl (B1) structure, in which the coordination number is six. Only three compounds (CsCl, CsBr, and CsI), adopt the CsCl (B2) structure where the coordination number is eight. Under pressure the B1 alkali-metal halides transform to the B2 phase,¹ while CsCl transforms from B2 to B1 above 742 K (Ref. 2). The relative stability between the B1 and B2 phases is textbook material and is conventionally explained using simple ionic models or radius ratio rules.³ It is therefore somewhat ironic that conventional density functional theory (DFT) calculations, based on the widely used generalized gradient approximation (GGA), do not predict that CsCl adopts the phase that bears its name, with instead the rocksalt B1 structure being favored. In this manuscript we explore this unexpected behavior, which is also shared by CsBr and CsI.

The energetic balance between competing phases in the alkali-metal halides has been studied for the best part of a hundred years. As far back as the 1930s it was reported by Born and Mayer^{4,5} and London⁶ that an accurate description of the stability of the CsCl-type structure for CsCl, CsBr, and CsI required the treatment of both zero point energy effects and dispersion, with the latter contributing around 1%–5% of the lattice energy. Although a small fraction of the total binding energy, this difference may be sufficient to explain the transition from the NaCl- to CsCl-type structure. Given that standard exchange-correlation functionals that depend only on the density and its first derivative at a single point in space are unable to capture the van der Waals (vdW) interactions that arise from dynamical correlation, this may explain this incorrect prediction.

There have been a number of theoretical studies of the competition between the B1-B2 structures for simple binary salts.^{7–14} Many of these studies have employed approximate methods, rather than a full quantum mechanical treatment. For example, the self-consistent atomic deformation method⁸

has been employed to compute the relative energy of these two structures for the alkali-metal halides. This approach was found to give a lower energy for the B1 structure in all cases. While this is correct for the majority of alkali-metal halides, it is naturally in error for CsCl, CsBr, and CsI. In the case of CsCl, the B1 structure was favored over B2 by 0.10 eV (Ref. 8). This is only a marginal quantitative improvement over a previous spherical ion result (0.13 eV) obtained by Cortona.⁹ Further investigations examined whether treating the heavier Cs ions relativistically would improve the result, but this failed to alter the finding.¹⁰

Pyper has suggested¹¹ that dispersion plays an important role in stabilizing the B2 phase in CsCl, and his most recent calculations¹² using the relativistic integrals program^{15,16} predict that the B2 phase is 0.078 eV/f.u. more stable than B1. The importance of dispersion has been questioned by Florez *et al.*¹³ who performed *ab initio* perturbed ion (APII) calculations^{17,18} on CsCl and found the correct phase ordering without taking explicit account of dispersion. However, these calculations incorrectly predicted that RbF and CsF also prefer the B2 structure, rather than the B1 phase seen experimentally. A later study on CsCl using the APII method and improved functionals by Aguado¹⁴ found an energy difference of approximately 0.14 eV/f.u. in favor of B2, but the predicted lattice constant was 3% larger than the experimental value extrapolated to zero Kelvin.

Given the broad success and computational feasibility of DFT for many problems, the failure of many current exchange-correlation functionals to properly describe dispersion interactions has been a significant limitation, at least quantitatively. Consequently, there has been considerable recent interest in approaches that make some allowance for long-range dispersive interactions within the framework of a DFT calculation. One approach is to use an explicitly nonlocal exchange-correlation functional that depends on the density and its gradient simultaneously at two points in space. This allows the asymptotic two-body limit of a $1/r^6$ interaction to be recovered, though it should be noted that this is not appropriate for all systems.^{19–21} Alternatively, Grimme²² has advocated a

semiempirical approach in which the dispersion contributions are additively included into a standard DFT calculation in the manner of an interatomic potential. Critical to this approach is that the dispersion contribution is damped at short range to avoid duplicating contributions that are captured by the exchange-correlation functional. A number of parametrizations have been proposed by Grimme for the combination of DFT calculations employing the generalized-gradient approximation (GGA) with supplementary dispersion terms. The original DFT + D (Ref. 23) and DFT + D2 (Ref. 22) employed empirical dispersion coefficients and interpolation formulas while the more recent DFT + D3 method (Refs. 24 and 25) uses an *ab initio* approach to calculate the dispersion coefficients. Of these various methods, the DFT + D2 approach is the most widely used. Recently the DFT + D3 method was privately implemented²⁶ but is not yet publicly available. Beyond these methods there are many alternative dispersion corrections, including those of Becke, Johnson,^{27,28} and co-workers who have derived schemes to determine the dispersion parameters for any system, including solids, from the properties of the exchange hole.

In this work we examine the influence of dispersion interactions on the relative energetics of the B1 and B2 structures using Grimme's DFT + D2 method. Currently the literature parametrization does not include elements from cesium onwards and so the appropriate dispersion parameters must first be derived. Following this we examine whether the lack of long-range dispersion interactions might indeed be the reason for the failure of current GGA calculations to correctly predict that cesium chloride should adopt the CsCl structure.

II. METHODOLOGY

All calculations have employed Kohn-Sham density functional theory (DFT) as implemented within the Vienna *ab initio* simulation package (VASP).^{29,30} The effective potential due to the core electrons and nucleus combined was described using the projector augmented wave (PAW) method.³¹ The PAW potentials used here have nine valence electrons for Cs and seven valence electrons for F, Cl, Br, and I. Convergence tests showed that kinetic energy cut-offs of 550 eV for CsF and 500 eV for CsCl, CsBr, and CsI, were sufficient for the plane-wave expansion of the valence electron wave functions. The auxiliary grid that is used to expand the electron density and augmentation charges employed a kinetic energy cutoff that was four times that of the wave function. For the exchange-correlation functional both the local density approximation (LDA) and generalized gradient approximation (GGA) of Perdew-Burke-Ernzerhof (PBE)³² were used. Sampling of the Brillouin zone was performed using a k -point mesh constructed according to the Monkhorst-Pack scheme. Here k -point meshes of $10 \times 10 \times 10$ and $6 \times 6 \times 6$ were used for the cesium chloride (B2) and rocksalt (B1) structures, respectively. During structural relaxation of each phase, all cell parameters and internal atomic positions were simultaneously relaxed. In all cases the total electronic energy was converged to better than 10^{-7} eV within the self-consistent field, while the geometry optimization was considered to be converged when the energy change between minimization steps was less than 10^{-6} eV. Cohesive energies were determined by combining the

bulk energy with spin-polarized atomic reference calculations for the constituent neutral species.

The long-range dispersion (van der Waals) contribution was described using the pragmatic DFT + D2 approach of Grimme,²² which involves adding a semiempirical dispersion term to the conventional Kohn-Sham³³ DFT energy:

$$E_{\text{DFT+D2}} = E_{\text{DFT}} + E_{\text{dispersion}}. \quad (1)$$

This dispersion contribution takes the following explicit form:

$$E_{\text{dispersion}} = -s_6 \sum_{i=1}^{N_{at}-1} \sum_{j=i+1}^{N_{at}} f(r_{ij}) \times \frac{C_6^{ij}}{r_{ij}^6}, \quad (2)$$

where s_6 is a global scaling factor that only depends on the density functional used (taking the value $s_6 = 0.75$ for PBE; Ref. 22), N_{at} is the number of atoms in the system, C_6^{ij} is the dispersion coefficient for the atom pair ij , and r_{ij} is the interatomic distance. The term $f(r_{ij})$ is a damping function that avoids the $r \rightarrow 0$ singularity and also removes the contribution from the empirical dispersion term in the regions where the exchange-correlation contribution is large and thereby reduces duplication of any short-range van der Waals contributions. The function $f(r_{ij})$ takes the form,

$$f(r^{ij}) = \frac{1}{1 + e^{-d(r^{ij}/R_0^{ij}-1)}}, \quad (3)$$

where R_0^{ij} is the sum of the atomic vdW radii. In the DFT + D2 formalism the value of the damping parameter d is 20.0 and the cutoff radius for the pairwise interactions is 30.0 Å. In order to facilitate general applicability without having to parametrize each specific interaction, the following combination rules are used to generate the pairwise dispersion coefficients C_6^{ij} and vdW radii R_0^{ij} :

$$C_6^{ij} = \sqrt{C_6^i \cdot C_6^j} \quad (4)$$

and

$$R_0^{ij} = R_0^i + R_0^j. \quad (5)$$

When the DFT + D2 method was proposed, the van der Waals parameters C_6 and R_0 were only determined for the elements of the first five rows of the periodic table. Accordingly, we first need to extend this parametrization to include appropriate values of C_6 and R_0 for Cs, as will be described in the next section.

III. RESULTS

A. Derivation of parameters

There are several methods in the literature that have been used to compute the van der Waals parameters required for the empirical dispersion correction of density functional theory. For example, time-dependent density functional theory can be used to determine the properties of atoms within specific crystalline structures.³⁴ In the present work we adhere to the structure-independent approach proposed by Grimme. In the original DFT + D scheme the atomic C_6 coefficients were taken from the work of Wu and Yang³⁵ and averaged over the possible hybridization states of the atoms. The errors

due to the use of atomic instead of hybridization-dependent C_6 coefficients were later estimated by Grimme²² to be on the order of 10%–20% of the binding energy. In order to obtain C_6 parameters for larger portions of the periodic table in a consistent manner, he proposed a simple computational scheme for atomic C_6 coefficients in the updated DFT + D2 version. In this new scheme, the C_6 parameter is derived from the London formula for dispersion and is based on the atomic ionization potentials (I_p) and static dipole polarizabilities (α). The C_6 coefficient (in units of $\text{J nm}^6 \text{mol}^{-1}$) for a single atom is then given as;

$$C_6 = 0.05 \times N I_p \alpha, \quad (6)$$

where I_p and α are in atomic units (i.e., Hartrees and Bohr, respectively) and N is the number of electrons for the noble gas atom from the same row. Accordingly, N has the value 2, 10, 18, 36, 54, and 86 for atoms in rows 1 through 6 of the periodic table, respectively.

In Grimme's DFT + D2 scheme, the C_6 parameters were calculated based on DFT/PBE0 calculations of atomic ionization potentials I_p and static dipole polarizabilities α . To reproduce binding energies and bond lengths of the lighter elements and noble gas systems, the proportionality constant in Eq. (6) was adjusted. However, this approach provided a poor definition of C_6 for elements from Group I, Group II, and the transition metals due to significant differences between the free atom and the atom as found in typical bonding environments. Accordingly, Grimme chose to treat atoms in Groups I and II by averaging the C_6 coefficient of the preceding noble gas atom with the following Group-III element. Naturally, this approach cannot be employed for Cs as there is no subsequent Group-III value available.

In our approach to estimating C_6 for Cs, we applied Eq. (6) to all Group-I elements using the first and second ionization potential I_p and the corresponding atomic and ionic polarizabilities (α) to describe neutral and single ionized atoms, respectively. The resulting C_6 parameters are listed in Table I; also shown in the table are the C_6 parameters from the DFT + D2 scheme.²² A graphical comparison between the

TABLE I. Comparison between dispersion coefficients C_6 computed using Eq. (6) and available DFT + D2 values in Ref. 22. Calculated data for both neutral and singly ionized cations is shown. All C_6 values are expressed in units of $\text{J nm}^6 \text{mol}^{-1}$. The quantity N is defined in the text. Ionization potential data (I_p) are from Ref. 36. Polarizability data (α) are from Ref. 37.

Species	N	I_p (eV)	α (a.u.)	C_6 (This work)	C_6 (Grimme)
Li	10	5.39	163.98	16.25	1.61
Li ⁺	10	75.64	0.19	0.27	
Na	18	5.14	159.26	27.067	5.71
Na ⁺	18	45.28	1.00	1.57	
K	36	4.34	292.87	84.09	10.80
K ⁺	36	31.63	5.40	11.17	
Rb	54	4.18	319.19	132.28	24.67
Rb ⁺	54	27.29	9.08	24.57	
Cs	86	3.89	402.19	247.47	
Cs ⁺	86	23.11	15.81	57.74	

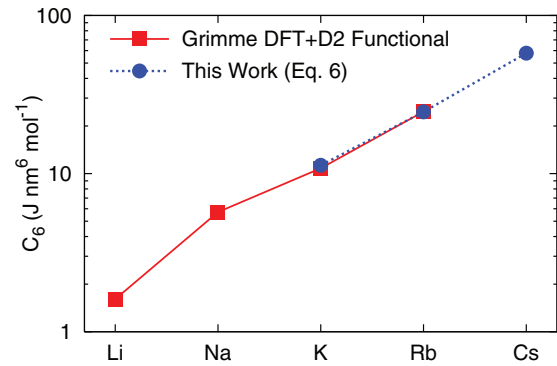


FIG. 1. (Color online) Comparison between selected Group-I dispersion coefficients calculated in this work and those in the Grimme DFT + D2 functional. The values taken in the present work are those for ionized cations, as listed in Table I.

DFT + D2 values and our own computed values of C_6 for ionized cations is provided in Fig. 1. For the heavier cations (K^+ and Rb^+), our computed C_6 values for ionized cations are strikingly close to those reported by Grimme. This is an important observation as it provides a strategy for estimating C_6 for Cs. Also apparent from this table is a large difference in C_6 between the neutral and ionized cases, with the former being much higher than those reported by Grimme. This behavior is consistent with Grimme's observation that neutral atoms are an inappropriate reference point when calculating C_6 values from atoms in many bonding environments. For the lighter cations (Li^+ and Na^+) our calculated values deviate from those of Grimme, but this difference is peripheral to this work as the important behavior is the trend for heavy elements. Taking the second ionization potential of Cs ($I_p = 23.11$ eV) [Ref. 36] and the polarizability of the Cs^+ cation ($\alpha = 15.18$ a.u.) (Ref. 37), leads to a calculated value of $C_6 = 57.74 \text{ J nm}^6 \text{mol}^{-1}$ for Cs. This value is used throughout the remainder of this manuscript.

As a general comment we note that Fig. 1 shows the expected trend in which C_6 increases with atomic number due to the lower effective nuclear charge experienced by the valence electrons, making them more polarizable. As a result, dispersion plays an increasingly important role in the phase stability of compounds as one moves down Group I. An example of this importance can be seen in a recent DFT/GGA study of pressure-induced ($\text{B1} \rightarrow \text{B2}$) phase transitions in rubidium halides.³⁸ The calculated transition pressures are significantly larger (typically by a factor of four) than experimental values, a discrepancy that may well be due to the absence of dispersion interactions in the DFT scheme. Indeed, in earlier interionic force calculations on the same system by Cohen and Gordon,³⁹ they pointed out that if the dispersion contributions could be incorporated into their calculations, they would have been likely to have obtained better agreement with experiment.

In Grimme's DFT + D and DFT + D2 functionals the van der Waals radius employed in the damping function (R_0) was determined for each element using the 0.01 a.u. electron density contour in ROHF/TZV calculations of atoms in their electronic ground state. This contour value was scaled by a factor of 1.22 in DFT + D and 1.10 in DFT + D2. To determine

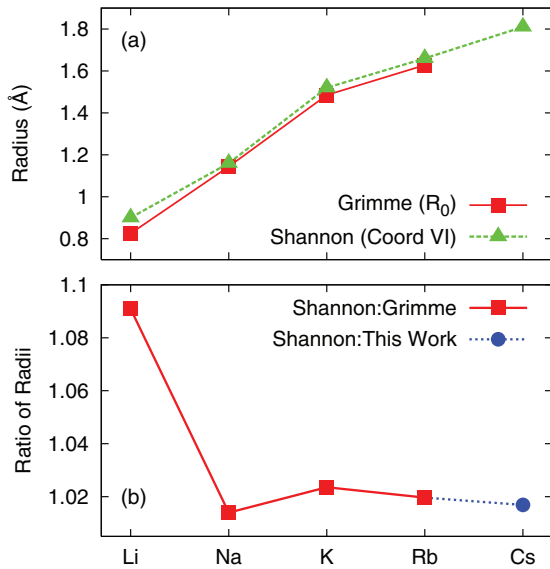


FIG. 2. (Color online) Graphical representation of (a) the data shown in Table II demonstrating the close relationship between the R_0 parameter in the DFT + D2 formalism (red squares) and the Shannon ionic radius for six-coordinate cations (green triangles), and (b) the ratio of the Shannon radii to Grimme R_0 values (red squares). The blue circle denotes the ratio corresponding to the estimated value of R_0 for Cs that is used in this work.

a value of R_0 for Cs, we first compared the R_0 values for Li, Na, K, and Rb from DFT + D2 against standard ionic radii.⁴⁰ Since the ionic radius is a function of the coordination number, it is necessary to standardize on a consistent environment. Although the CsCl structure involves eightfold coordination, it is more reasonable to choose sixfold radii as a reference, given that octahedral environments predominate amongst the Group-I halides.

As shown in Fig. 2(a), there is a close correlation between the Shannon ionic radii and the values of R_0 used in the DFT + D2 method. Figure 2(b) and Table II present the ratio between R_0 and the six-coordinate Shannon ionic radius for the Group-I elements. It can be seen that the Shannon radii and Grimme R_0 values are largely close to each other with the former being slightly larger by a near constant ratio. In this regard, Li^+ is somewhat the exception with a marginally greater difference between the values. Excluding this element,

TABLE II. Comparison between the damping function parameter (R_0) in the DFT + D2 approach²² and Shannon ionic radii⁴⁰ for six-coordinate cations. The DFT + D2 data are for Li-Rb, while the Shannon data are for Li-Cs. The value of R_0 for Cs is estimated as described in the text by scaling the Shannon radius by a factor of 1.019.

Element	R_0 (Å)	Shannon (VI) (Å)	Ratio
Li	0.825	0.90	1.091
Na	1.144	1.16	1.014
K	1.485	1.52	1.024
Rb	1.628	1.66	1.020
Cs	1.776 ^a	1.81	1.019

^aThis work

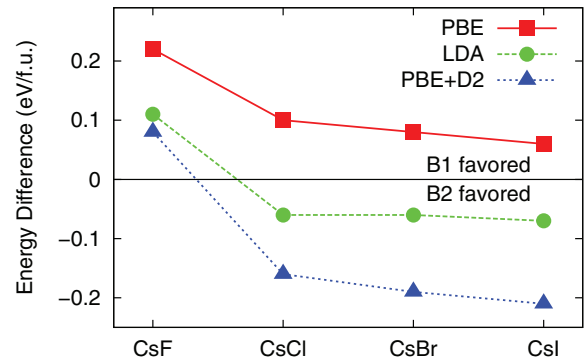


FIG. 3. (Color online) Energy differences (eV/f.u.) between the B1 and B2 phases of CsX ($X = \text{F}, \text{Cl}, \text{Br}, \text{I}$) calculated using LDA (circles), PBE (squares), and PBE + D2 (triangles) functionals.

the ratio of the Shannon ionic radii to Grimme R_0 is 1.019 ± 0.005 for Na^+ , K^+ , and Rb^+ . Based on this average ratio for the heavier Group-I cations, we have estimated the R_0 value for Cs to be 1.776 Å. According to Grimme's philosophy,²² a Group-II element has the same C_6 and R_0 values as that of the Group-I element in the same row. Consequently, the parameters determined here for Cs can also be applied to barium.

B. Application to cesium halides

Using the fitted C_6 and R_0 parameters values for Cs^+ and the available parameters for the halogens,²² we performed both standard (LDA and PBE) and DFT + D2 dispersion-corrected PBE calculations for the cesium halides (CsF , CsCl , CsBr , and CsI). In the following we will denote the latter calculations as PBE + D2 to emphasize the functional employed. Figure 3 shows the energy difference between the B1 and B2 phases of Cs halides as calculated at the LDA, PBE and PBE + D2 levels; the quantitative values are listed in Table III along with the cohesive energies. The energy difference ΔE is defined such that a positive value indicates the B1 structure is favored, while conversely a negative value indicates that B2 is favored. Although the LDA approach is generally less accurate than GGA, typically overbinding in comparison with experiment, here it successfully predicts the experimentally observed phase for all of the Cs halide compounds. The same is true for the PBE + D2 calculations, which show a small systematic shift relative to the LDA energetics in favor of the B2 phase. At the PBE level, however, all four Cs halides are predicted to adopt the rocksalt B1 phase. In other words, calculations at the PBE/GGA level do not predict that CsCl adopts the CsCl structure. The same error is seen for CsBr and CsI, which also adopt the B2 phase under ambient conditions. We note that our energy differences for CsCl using the LDA and PBE + D2 functionals are similar to those calculated by Pyper¹² and Aguado¹⁴ who reported values of 0.078 and 0.14 eV/f.u., respectively,

Cohesive energies calculated using the PBE + D2 functional (Table III) compare very well with experiment⁴¹ for the B2 phases where the difference is less than 0.16 eV/f.u. This performance is superior to the other two functionals examined which have larger discrepancies; for LDA the maximum discrepancy for B2 phases is 0.30 eV/f.u., while for PBE it is

TABLE III. Cohesive energies (eV/f.u.) for the B1 and B2 phases of CsX ($X = \text{F, Cl, Br, I}$) calculated using LDA, PBE, and PBE + D2 functionals. The energy difference ΔE is defined in the text. The experimentally preferred phases are B1 for CsF and B2 for CsCl, CsBr, and CsI. This trend is reproduced by the LDA and PBE + D2 functionals, but not with PBE.

Structures	B1 (NaCl)	B2 (CsCl)	ΔE
CsF			
LDA	-8.24	-8.13	0.11
PBE	-7.19	-6.97	0.22
PBE + D2	-7.94	-7.86	0.08
Experiment ⁴¹	-7.48		
CsCl			
LDA	-6.89	-6.94	-0.06
PBE	-6.13	-6.04	0.10
PBE + D2	-6.68	-6.84	-0.16
Experiment ⁴¹		-6.74	
CsBr			
LDA	-6.39	-6.45	-0.06
PBE	-5.68	-5.60	0.08
PBE + D2	-6.29	-6.48	-0.19
Experiment ⁴¹		-6.48	
CsI			
LDA	-5.80	-5.88	-0.07
PBE	-5.13	-5.07	0.06
PBE + D2	-5.81	-6.02	-0.21
Experiment ⁴¹		-6.18	

substantially greater at 1.11 eV/f.u. In contrast, none of the functionals predict the cohesive energy particularly accurately for the B1 phase of CsF, with PBE being the closest.

The relative importance of dispersion can be quantified from Table III by comparing the cohesive energies of the PBE and PBE + D2 calculations. This energy difference is surprisingly invariant, falling in the range of 0.55–0.75 eV/f.u. for the B1 structures and 0.80–0.95 eV/f.u. for the B2 structures; the average values are 0.65 and 0.88 eV/f.u., respectively. There is no apparent trend down the group, suggesting that the increasing C_6 coefficient associated with a higher atomic number is counteracted by the larger lattice parameter. Accordingly, the dispersion contribution to the cohesive energy is roughly constant for a given structure type. We note that the average dispersion contribution in the B2 structures is larger than its B1 equivalent by a ratio of 8:6, which matches that of the coordination numbers of the two structures.

Although the dispersion force is comparatively weak, it is always attractive and hence its inclusion always decreases the cell volume. This behavior is evident in Fig. 4 which plots cell volumes for the B1 and B2 phases of the cesium halides at 0 K. Experimental values for the cell volumes at 0 K were corrected from the lowest measured temperature (293 K for CsF, 5 K for CsCl, and 20 K for CsBr and CsI) using experimental thermal expansion data.^{42,43} In the case of the B1-CsCl phase the experimental value at 450 K was corrected to 0 K by assuming that this phase has the same thermal expansion coefficient as the B2 phase. Whereas the PBE functional consistently overestimates the volume (by an average of 9%), the LDA

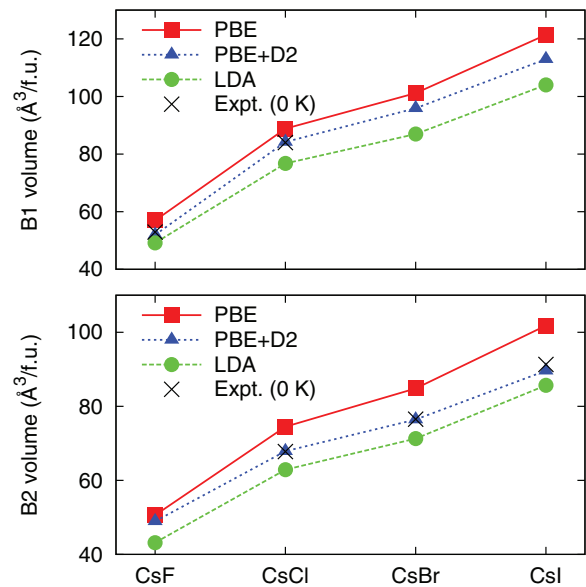


FIG. 4. (Color online) Cell volumes ($\text{\AA}^3/\text{f.u.}$) for the B1 and B2 phases of CsX ($X = \text{F, Cl, Br, I}$) calculated using LDA (circles), PBE (squares), and PBE + D2 (triangles) functionals. Experimental values (crosses) for the cell volumes were corrected from the lowest measured temperature to 0 K using the available thermal expansion data (see text for details).

functional conversely underestimates the same quantity (by an average of 7%). In every case the PBE + D2 functional provides an excellent prediction of the cell volume with an average difference of only 0.9%. Furthermore, the PBE + D2 results are far closer to the extrapolated experimental values at 0 K than those obtained in calculated by Aguado¹⁴ and Pyper¹² for which the cell volume at zero Kelvin is overestimated by 8.7 and 5.3%, respectively.

C. Sensitivity analysis

Given that the parameters C_6 and R_0 are empirically determined, it is instructive to perform a sensitivity analysis of their effects. For this we have chosen to focus on the compound CsCl, using the lattice parameter of the B2 phase and the energy difference between the B1 and B2 phases to highlight the effect of varying C_6 (Fig. 5) and R_0 (Fig. 6). The vertical dashed line in each figure indicates the parameter value used elsewhere in this work. Also included in Figs. 5(a) and 6(a) using solid horizontal lines are the experimental lattice parameter at both 300 K and 0 K, which is corrected using the available thermal expansion data, and the value computed by Pyper.¹² The B1-B2 energy difference calculated by Pyper¹² and Aguado¹⁴ is also shown, with the latter being closer to our PBE + D2 result of 0.16 eV/f.u. Both the lattice parameter and the B1-B2 energy difference demonstrate great sensitivity to the choice of C_6 and R_0 parameters, as would be expected. When either C_6 increases or R_0 decreases, the dispersion forces become stronger, which increases the binding in CsCl and makes the B2 phase more stable than the B1 structure. Our C_6 and R_0 parameters for Cs in the DFT + D2 calculations are obtained independently and rely only on the physical properties of the Cs cation. By employing these parameter values, the calculated cell lattice parameter of

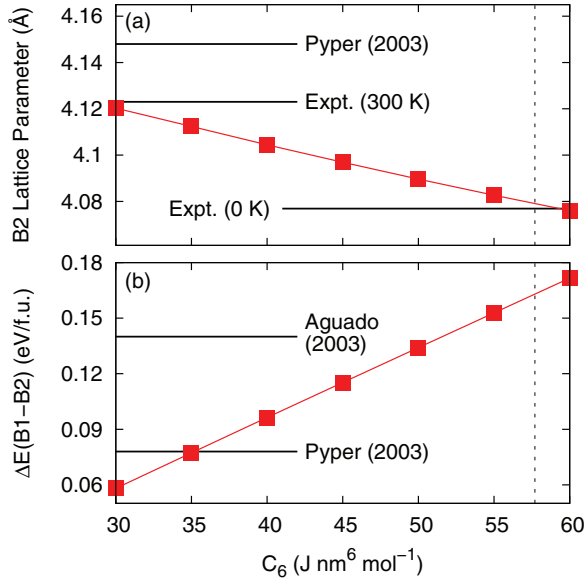


FIG. 5. (Color online) C_6 ($\text{J nm}^6 \text{mol}^{-1}$) sensitivity analysis for (a) CsCl lattice parameter (\AA) and (b) its energy difference between B1 and B2 phases ΔE (eV/f.u.). Also shown are experimental lattice parameters at 0 K and 300 K, and the values of (a) the lattice parameter and (b) the energy difference computed by Pyper.¹² Panel (b) also shows the energy difference computed by Aguado¹⁴ but for clarity the predicted B2 lattice parameter of 4.192 \AA is not shown in panel (a). The experimental value at 0 K is obtained as described in the text. R_0 is fixed as 1.776 \AA . The dashed vertical line represents the value (57.74 $\text{J nm}^6 \text{mol}^{-1}$) we used in this work.

B2-CsCl happens to be very close to that of the experimental value extrapolated to 0 K. While this represents a useful further validation of our choice of parameters, it should be noted that

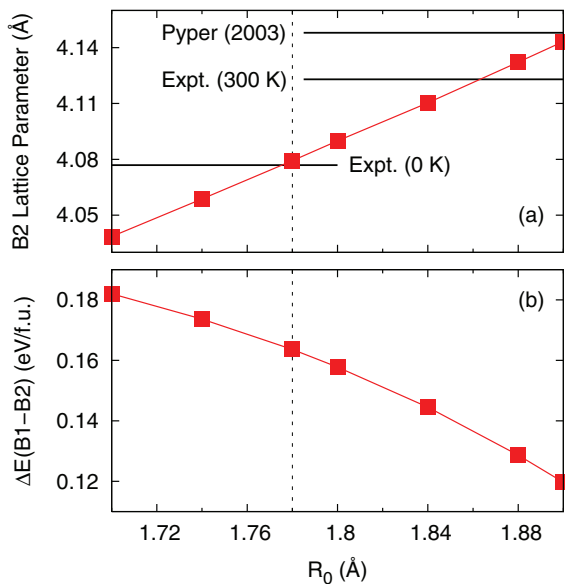


FIG. 6. (Color online) R_0 (\AA) sensitivity analysis for (a) CsCl lattice parameter (\AA) and (b) its energy difference between B1 and B2 phases ΔE (eV/f.u.). Also shown are experimental lattice parameters at 0 K and 300 K, and the values computed by Pyper.¹² C_6 is fixed at 57.74 $\text{J nm}^6 \text{mol}^{-1}$. The dashed vertical line indicates the value (1.776 \AA) used in this work.

the DFT + D2 should formally be corrected for zero point energy effects in order to equate it to the experimental value at absolute zero. However, for the relatively heavy atoms present in CsCl it is unlikely that the zero point vibration will lead to a substantial expansion of the unit cell.

An alternative strategy to obtain values for R_0 and C_6 would have been to fit the parameters to the available experimental properties. However, given that the present systematic approach has managed to deliver both physically reasonable structures and phase stabilities, this would have been less satisfying and may have led to a less transferable parametrization.

IV. DISCUSSION AND CONCLUSIONS

In this work, we have examined the failure of density functional theory based on a widely used generalized gradient approximation, namely PBE, to correctly predict that CsCl should adopt the cesium chloride structure at standard conditions. Although not exhaustively examined, we strongly suspect that this failure will also occur with other GGA exchange-correlation functionals in the literature. Given that the local density approximation yields the correct result, the overestimation of volume is clearly correlated with the error in the relative phase energies. As nearly all GGA functionals similarly underestimate the binding of solids, it appears reasonable that the failure will be widespread. It might be expected that the family of GGA functionals that are specifically parametrized for solids or from the Airy gas, such as Wu-Cohen⁴⁴ and AM05,⁴⁵ respectively, could give improved results. Hence we have tested the performance of a solid-state parameterized GGA, namely PBEsol,⁴⁶ for the B1-B2 energy difference in the case of CsCl. While the relative energy is reduced to 0.03 eV/f.u. with this functional, as compared to 0.10 eV/f.u. from PBE, the result remains qualitatively incorrect.

As a result of the erroneous predictions arising from the use of GGA functionals alone, we have examined the influence of including semiempirical long-range dispersion via the DFT + D2 methodology of Grimme and co-workers. Although the dispersion energy corrections are small as a fraction of the overall cohesive energy, we find that it plays a vital role in determining the phase stability of CsCl, CsBr, and CsI. The importance of the dispersion correction can also be seen in the results of calculations using a wide range of functionals, including PBEsol, the screened hybrid, HSE06 (Ref. 47), and also the hybrid functional, PBE0 (Ref. 48). Table IV presents the energy difference ΔE between B1- and B2-type CsCl as

TABLE IV. The energy difference ΔE (eV/f.u.) between B1- and B2-type CsCl calculated by using the exchange-correlation functionals PBEsol, HSE06, and PBE0. ΔE is defined as B2-B1, such that a positive value indicates the B1 structure is favored, while conversely a negative value indicates that B2 is favored.

Functional	PBEsol	HSE06	PBE0
ΔE Without D2	0.028	0.082	0.077
ΔE With D2	-0.194	-0.225	-0.231

determined using PBEsol, HSE06, and PBE0. All of these functionals exhibit the same qualitative result as for PBE, i.e., the incorrect order of stability for CsCl. Addition of dispersion corrections to any of these functionals leads to the correct order of phase stability, thereby showing that dispersion is indeed the single most important factor.

In the present work the C_6 and R_0 parameters for cesium in the dispersion correction have been empirically determined based on a combination of theoretical arguments and extrapolation of data for the alkali-metal cations. Importantly, no specific reference is made to the target cesium halide structures to which the parameters have been applied. Despite this, and the demonstrated sensitivity of the results to the choice of dispersion parameters, the values determined here (i.e., 57.74 J nm⁶mol⁻¹ for C_6 and 1.776 Å for R_0) give not only the correct relative phase stabilities, but also superior lattice parameters relative to the other functionals examined. With one exception, the cohesive energies are also in improved agreement with the experimental values. Finally, we also note

that the magnitude of the dispersion energy contribution for the cesium halides does not exhibit a systematic variation with size or atomic number of the ions, although the underlying C_6 and R_0 parameters obviously do. It appears that the increased lattice parameter for larger ions offsets the corresponding increase in polarizability. Instead, the crucial factor that corrects the relative stability of the B1 and B2 phases is that the total dispersion energy is found to be proportional to the first coordination number of the structure, which is sufficient for CsCl to favor the cesium chloride structure, just as we would expect.

ACKNOWLEDGMENTS

We gratefully acknowledge financial support from the US Department of Energy through the LANL/LDRD program. J.D.G. and N.A.M. both thank the Australian Research Council for fellowships and iVEC and National Computational Infrastructure for provision of computing resources.

*f.zhang@curtin.edu.au

¹C. W. Pistorius, *Prog. Solid State Chem.* **11**, 1 (1976).

²J. Shanker and M. Kumar, *Phys. Status Solidi (b)* **158**, 11 (1990).

³W. B. Jensen, *Journal of Chemical Education* **87**, 587 (2010).

⁴M. Born and J. E. Mayer, *Zeitschrift für Physik A Hadrons and Nuclei* **75**, 1 (1932).

⁵J. E. Mayer, *J. Chem. Phys.* **1**, 270 (1933).

⁶F. London, *Trans. Faraday Soc.* **33**, 8b (1937).

⁷J. Narain, N. K. Dwivedi, G. G. Agrawal, and J. Shanker, *Phys. Status Solidi (b)* **132**, 389 (1985).

⁸W. N. Mei, L. L. Boyer, M. J. Mehl, M. M. Ossowski, and H. T. Stokes, *Phys. Rev. B* **61**, 11425 (2000).

⁹P. Cortona, *Phys. Rev. B* **46**, 2008 (1992).

¹⁰J. M. Recio, A. M. Pendás, E. Francisco, M. Flórez, and V. Luaña, *Phys. Rev. B* **48**, 5891 (1993).

¹¹N. C. Pyper, *Chem. Phys. Lett.* **220**, 70 (1994).

¹²N. C. Pyper, *J. Chem. Phys.* **118**, 2308 (2003).

¹³M. Flórez, J. M. Recio, E. Francisco, M. A. Blanco, and A. M. Pendás, *Phys. Rev. B* **66**, 144112 (2002).

¹⁴A. Aguado, *J. Chem. Phys.* **119**, 8765 (2003).

¹⁵C. Wood and N. Pyper, *Chem. Phys. Lett.* **81**, 395 (1981).

¹⁶C. Wood and N. Pyper, *Philos. Trans. R. Soc. A: Physical, Mathematical and Engineering Sciences* **320**, 71 (1986).

¹⁷V. Luaña and L. Pueyo, *Phys. Rev. B* **41**, 3800 (1990).

¹⁸M. A. Blanco, A. M. Pendás, and V. Luaña, *Comput. Phys. Commun.* **103**, 287 (1997).

¹⁹G. Román-Pérez and J. M. Soler, *Phys. Rev. Lett.* **103**, 096102 (2009).

²⁰M. Dion, H. Rydberg, E. Schröder, D. C. Langreth, and B. I. Lundqvist, *Phys. Rev. Lett.* **92**, 246401 (2004).

²¹J. F. Dobson, A. White, and A. Rubio, *Phys. Rev. Lett.* **96**, 073201 (2006).

²²S. Grimme, *J. Comp. Chem.* **27**, 1787 (2006).

²³S. Grimme, *J. Comput. Chem.* **25**, 1463 (2004).

²⁴S. Grimme, J. Antony, S. Ehrlich, and H. Krieg, *J. Chem. Phys.* **132**, 154104 (2010).

²⁵S. Grimme, S. Ehrlich, and L. Goerigk, *J. Comput. Chem.* **32**, 1456 (2011).

²⁶W. Reckien, F. Janetzko, M. F. Peintinger, and T. Bredow, *J. Comput. Chem.* **33**, 2023 (2012).

²⁷A. D. Becke and E. R. Johnson, *J. Chem. Phys.* **122**, 154104 (2005).

²⁸A. D. Becke and E. R. Johnson, *J. Chem. Phys.* **127**, 154108 (2007).

²⁹G. Kresse and J. Furthmüller, *Phys. Rev. B* **54**, 11169 (1996).

³⁰G. Kresse and J. Furthmüller, *Comput. Mater. Sci.* **6**, 15 (1996).

³¹P. E. Blöchl, *Phys. Rev. B* **50**, 17953 (1994).

³²J. P. Perdew, K. Burke, and M. Ernzerhof, *Phys. Rev. Lett.* **77**, 3865 (1996).

³³W. Kohn and L. J. Sham, *Phys. Rev.* **140**, A1133 (1965).

³⁴G.-X. Zhang, A. Tkatchenko, J. Paier, H. Appel, and M. Scheffler, *Phys. Rev. Lett.* **107**, 245501 (2011).

³⁵Q. Wu and W. Yang, *J. Chem. Phys.* **116**, 515 (2002).

³⁶J. E. Huheey, *Inorganic Chemistry: Principles of Structure and Reactivity*, 3rd ed. (Harper and Row, New York, 1983).

³⁷S. Hati and D. Datta, *J. Phys. Chem.* **99**, 10742 (1995).

³⁸K. Haddadi, A. Bouhemadou, L. Louail, and D. Maouche, *Phase Transitions* **82**, 266 (2009).

³⁹A. J. Cohen and R. G. Gordon, *Phys. Rev. B* **12**, 3228 (1975).

⁴⁰R. D. Shannon, *Acta Crystallographica Section A* **32**, 751 (1976).

⁴¹M. Tosi, *Journal of Physics and Chemistry of Solids* **24**, 965 (1963).

⁴²G. K. White and J. G. Collins, *Proc. R. Soc. London A Mathematical and Physical Sciences* **333**, 237 (1973).

⁴³K. Wang and R. Reeber, *J. Appl. Crystallogr.* **28**, 306 (1995).

⁴⁴Z. Wu and R. E. Cohen, *Phys. Rev. B* **73**, 235116 (2006).

⁴⁵A. E. Mattsson and R. Armiento, *Phys. Rev. B* **79**, 155101 (2009).

⁴⁶J. P. Perdew, A. Ruzsinszky, G. I. Csonka, O. A. Vydrov, G. E. Scuseria, L. A. Constantin, X. Zhou, and K. Burke, *Phys. Rev. Lett.* **100**, 136406 (2008).

⁴⁷A. V. Krukau, O. A. Vydrov, A. F. Izmaylov, and G. E. Scuseria, *J. Chem. Phys.* **125**, 224106 (2006).

⁴⁸C. Adamo and V. Barone, *J. Chem. Phys.* **110**, 6158 (1999).